A non-local approach to shape from ambient shading

Emmanuel Prados, Nitin Jindal, Stefano Soatto

INRIA

INSTITUT NATIONAL DE RECHERCHE EN INFORMATIQUE ET EN AUTOMATIQUE

A non-local approach to shape from ambient shading

Emmanuel Prados — Nitin Jindal — Stefano Soatto

N° 7783

November 2011

Thème COG

ISSN 0249-6399 ISRN INRIA/RR--7783--FR+ENG

INSTITUT NATIONAL
DE RECHERCHE
EN INFORMATIQUE
ET EN AUTOMATIQUE

INRIA

centre de recherche
GRENOBLE - RHÔNE-ALPES

A non-local approach to shape from ambient shading

Emmanuel Prados*, Nitin Jindal , Stefano Soatto†

Thème COG — Systèmes cognitifs
Équipes-Projets Perception

Rapport de recherche n° 7783 — November 2011 — 23 pages

Abstract: We describe a mathematical and algorithmic study of Shape From Shading problem for scenes illuminated by ambient lighting. The ambient lighting is here modelled by a (whole) spherical light source of infinite radius centered on the object of interest. The mathematical formulation of this problem results in resolving a strongly non-local and non-linear Integro-Partial Differential Equation (I-PDE). The first contribution of this report is to provide a first theoretical study of this global I-PDE, when previous theoretical works only deal with a local version obtained by ignoring the shadow, i.e. the occlusion of the light field by the surface itself. We give a comparison result in the C^1 space which allows to characterize the set of the solutions. The second contribution consists in providing a monotonic, consistent and stable approximation scheme for the I-PDE which, according to Barles and Souganidis' theory, classically ensures the correctness of the numerical approximations. We then explain how to implement the associated numerical algorithm and show and discuss about some numerical results. Contrary to our previous conference paper [26], this technical report contains the detailed proofs of all stated theorems.

Key-words: Shape From Shading, Ambient/Diffuse Lighting, Partial Differential Equation, Integro-PDE, PDE with Global Terms, Non-Local PDEs.

* STEEP Lab., INRIA Rhône-Alpes, France
† UCLA, USA

Centre de recherche INRIA Grenoble – Rhône-Alpes
655, avenue de l'Europe, 38334 Montbonnot Saint Ismier
Téléphone : +33 4 76 61 52 00 — Télécopie +33 4 76 61 52 52

Une approche non-locale au problème du "Shape From Shading" en éclairage diffus

Résumé : Nous présentons une première étude mathématique et un premier algorithme numérique rigoureux pour le problème du "Shape From Shading" dans le cas d'une scène éclairée uniquement par un éclairage ambiant (diffus). L'éclairage ambiant est ici modélisé par une source de lumière sphérique de rayon infini et centrée sur l'objet d'intérêt. La formulation mathématique de ce problème aboutit à la résolution d'une équation intégro-différentielle (équation aux dérivées partielles contenant un terme intégral) fortement non locale et non linéaire. Ce travail s'illustre par ses deux principales contributions. 1) Tout d'abord, nous fournissons une première étude théorique de cette équation globale, alors que les travaux théoriques précédents se limitaient à une version locale obtenue en ignorant les ombres portées, c'est à dire en ignorant les occlusions du champ de lumière par la surface elle même. Plus précisément, nous formulons un résultat de comparaison qui permet de caratcériser les solutions de classe C^1. 2) Ensuite nous fournissons un premier algorithme numérique qui vérifie rigoureusement les propriétés classiques de convergence (stabilité, cohérence, monotonie) développées par Barles et Souganidis. Nous expliquons ensuite comment implémenter notre algorithme et nous analysons quelques exemples de résultats numériques.

Mots-clés : Shape From Shading, éclairage ambient/diffus, équation aux dérivées partielles, équation integro-différentielle globale, EDP non-locale.

Note

This technical report has been mainly written in 2008. At that time, I expected to find some time to improve it a little bit. Nevertheless, because of a change of research field, I have never been able to work again on it. To publish this report is nevertheless important since it is the only document which contains the detailed proofs of the theoretical results we stated in our conference paper [26]. This is why I have finally decided to publish it even without real modifications.

Emmanuel.

1 Introduction

The Shape From Shading problem (SFS) is to compute the three-dimensional shape of a surface from the brightness of one black and white image of that surface. This problem having emerged as a quite intractable one, the authors had then naturally to simplify its modelling and so all the previous work attempting to provide solutions was based on very rudimentary assumptions. The simplifications and the poorness of the models run right through all the modelling components; in particular the reflectance properties, the lighting and the camera model. In this work we focus on lighting and we want to go beyond the classical light modelling which assumes that the scene is illuminated by a single far and punctual light source [32, 12, 21, 15]. In [25], Prados and Faugeras prove that the difficulties met in Shape From Shading are directly related to the simplicity of the models and not to some algorithmic bolts. More precisely, they prove that the ill-posedness of the Shape From Shading problem can be completely removed by changing the assumptions on lighting and its modelling. For obtaining such a result they consider a punctual and proximal light source and they take into account the attenuation of the light due to the distance. Thus any reasonable numerical method (i.e. rigorous enough) should return relevant approximations. Also, in a sense, here we propose a continuation of [25]: we want now to study the effect of the ambient lighting on the well-posedness of the SFS problem.

To our knowledge, at the exception of the work of Tian, Tsui and Yeung [28], the work of Langer et al. [18, 27, 17], the work of Lions, Rouy and Tourin [19], and the work [29, 20, 30], all the SFS papers assume that the scene is illuminated by punctual light sources.
Tian, Tsui and Yeung [28] propose a *numerical* SFS algorithm for dealing with some non-punctual and multiple light sources (any combination of spherical, rectangular and cylindrical light sources). Langer et al. [18, 27, 17] consider the case of *ambient lighting*. The even more daring work of [20, 29, 17, 30] proposes some methods allowing to deal with interreflection. In all these previous works [28, 18, 27, 17, 20, 29, 17], the authors do not consider at all the theoretical aspects of the problem (in particular the existence and the uniqueness of the solution).
At the extreme opposite, Lions, Rouy and Tourin [19] *theoretically study* the SFS problem for multiple and continuous distributed light sources. As Tian, Tsui and Yeung [28], Lions, Rouy and Tourin neglect the shadows (i.e. the occlusion of the light field

by the surface itself); more exactly, they assume that for any fixed point x on the surface, all the light sources located on the hemisphere normal to the surface at x are visible from this point. This allows them to remove the global nature of the equation they (initially) consider and this reduces quite significantly the difficulties of the theoretical study.
As Langer et al. [18, 27, 17] we focus here on *ambient lighting*. In their work, Langer et al. propose some numerical algorithms designed from simplified and heuristic models; they do not neglect the "shadows effect" and they model interreflections. They also underline the importance of ambient lighting in psychophysics. The ambient lighting is in effect dominant in common real scenes. In particular, this is the case for the famous "cloudy day" [18], but this is also roughly the case in most of the inside scene illuminated by windows with curtains, by a number of indirect light sources and when the inter-reflections on the walls are important. In this context, light comes from *all* directions and the assumption of Lions, Rouy and Tourin [19] is equivalent to assume that the solution is concave. Here, we do not want to limit ourself to concave shapes Then, for dealing with ambient lighting, we have to get rid of Lions' constraint which is too much restrictive from the computer vision point of view[1]. This yields in new and significant difficulties [from the theoretical as well as numerical point of view] that we fully brave. Thus, here, we provide an original theoretical result for the "Shape From Ambient Shading" problem. Also, contrary to the previous works, we provide a rigorous numerical algorithm verifying the properties of monotony, consistency and stability which typically ensure its convergence (see [4]).

The paper is organized as follows. In section 2, we describe the modeling assumptions and we specify the notations. In section 3 we formulate the Shape From Ambient Shading problem as a Partial Differential Equation (more exactly as an integro-differential equation). We develop our theoretical results in section 5 (comparison and uniqueness results). We describe our numerical algorithm and we study it in section 5. We show some experimental results on synthetic data sets in section 6. Some discussion and future work are given in section 7.

2 Modeling of The Problem

The Shape From Shading problem consists of exploiting the shading information to compute the three-dimensional shape of a surface. The shading is the result of a combination of the reflectance property of the scene (object of interest), of the lighting conditions, and of the geometry of the scene and of the camera. So in a sense recovering shape from shading consists of factorizing these four components. To exploit the shading information we have then to model the process of image formation; also we have to make some assumptions on all of these components (in particular on the reflectance, the lighting and the geometry of the camera; the geometry of the scene being the unknown).

2.1 Reflectance Assumptions

Let $\mathcal{S}$ be a *Lambertian* 2D surface manifold of $\mathbb{R}^3$ with a *constant albedo*. The Bidirectional Reflectance Distribution Function (*BRDF*) [14] of the surface S is then a

[1] For simplicity we nevertheless neglect the interreflection effects, as Lions et al. [19].

constant function which does not depend on the radiance direction (viewing direction) ν_{px}, on the light source direction ν and on the position of the considered point $p \in \mathcal{S}$:

$$\beta(p; \nu_{px}, \nu) = \rho.$$

$\rho \in \mathbb{R}$ is called the *albedo*. Without loss of generality we can assume that the albedo is equal to 1.

2.2 Lighting Assumptions

As in [18, 27, 17], we assume that the *scene is only illuminated by ambient lighting*.

Definition 2.1. [Ambient illumination] A power density distribution $R_L(\nu)d\nu$ defined for any ν in the unit sphere $\mathbb{S}^2$ of $\mathbb{R}^3$ is called *ambient illumination*.

We assume that the dominating sky principle holds [18]. In other words, we neglect inter-reflexions, and so, for any point of the surface the light irradiance only come from the (spherical) sky.
To simplify the problem, later we will also assume that the ambient illumination is homogeneous, that is to say, that the power density distribution is constant. As explained in section 2.3, this assumption is required if we want to get rid of other constraints while still keeping the problem reasonable and interesting. Without loss of generality we then will fix $R_L(\nu) = 1$.

Now, contrary to most of the previous work, we want to deal with scenes where the light field can be partly occluded by the object of interest itself. In other words, we assume that there are "self-shadows" and we want to take them into account. We then need to introduce the

Definition 2.2. [Light visibility] Let q be a point in $\mathbb{R}^3$. We call *visibility function* and we denote $\chi_{\mathcal{S}}(q; \nu)$ the indicator function of the directions $\nu \in \mathbb{S}^2$ from q that are not occluded by $\mathcal{S}$, i.e. the function

$$\chi_{\mathcal{S}}(q; \nu) = \begin{cases} 1 & \{q + \lambda\nu, \lambda \in \mathbb{R}_+\} \cap \mathcal{S} = \phi, \\ 0 & \text{otherwise.} \end{cases}$$

The set

$$\mathbf{C}_{\mathcal{S},q} = \{\nu \in \mathbb{S}^2 : \chi_{\mathcal{S}}(q; \nu) = 1\}$$

is called *visibility cone* at $q \in \mathbb{R}^3$.

The visibility function specifies if a point q is reached by the light ray of direction ν. If the 3D point q sees the light ray then $\nu\ \chi_{\mathcal{S}}(q; \nu) = 1$, else if this light ray is occluded by another part of the scene $\mathcal{S}$ then $\chi_{\mathcal{S}}(q; \nu) = 0$. The visibility cone assembles all the visible rays from a point q.

Let us note that we do not want to just take "self-shadows" into account but we want to exploit the information it provides to recover the shape of the scene. Somewhere there is then a link between our work and the previous papers on "shape From Shadows" [5, 6, 13, 11, 7, 31] which analyses the edges caused by shadows. But contrary to these papers, here, the lighting is only composed by a continuous distributed light source (the ambient lighting) without any punctual light source. Then here the lighting occlusions do not generate any edge in the imager; they just generate some continuous darkening.

2.3 Resulting Radiance

The surface being Lambertian (with $\rho = 1$) and illuminated by the ambient illumination $R_L(\nu)d\nu$, when we take into account the occlusions of the light field caused by the object itself, the radiance of the surface at point p is given by

$$R_{\mathcal{S}}(p) \quad = \quad \int_{\mathbb{S}^2} \chi_{\mathcal{S}}(p;\nu)\langle \nu, \nu_p\rangle R_L(\nu)\, d\nu \quad = \quad \int_{\mathbf{C}_{\mathcal{S},p}} \langle \nu, \nu_p\rangle\, R_L(\nu)\, d\nu, \quad (1)$$

where ν_p is the normalized normal vector to the surface S at the point p, see [14]. Here, the surface is implicitly assumed to be smooth. This ensures that all the light rays visible from a point come from above its tangent plane. So for all point p on the surface $\mathcal{S}$, all the light rays visible from that point are included in the hemisphere defined by the normal ν_p to the surface at that point; that is to say $\mathbf{C}_{\mathcal{S},p} \subset Hemi_{\nu_p}$. Therefore $\forall \nu \in \mathbf{C}_{\mathcal{S},p}$, $\langle \nu, \nu_p\rangle \geq 0$. To underline the fact that our radiance modeling would not make sense with edges, but also for mathematical conveniences, we will enforce this property in the radiance as:

$$R_{\mathcal{S}}(p) = \int_{\mathbf{C}_{\mathcal{S},p}} \langle \nu, \nu_p\rangle^+\, R_L(\nu)\, d\nu. \quad (2)$$

where for all a in $\mathbb{R}$, $a^+ = a$ if $a \geq 0$ and $a^+ = 0$ else.

At the stage, one can immediately see the difficulty generated by the fact that we take into account the occlusions of the light field caused by the object itself. In effect, the integration domain of (2) is reduced to the visibility cone $\mathbf{C}_{\mathcal{S},p}$ which directly depends of the whole scene $\mathcal{S}$. Then the radiance does not only depend on local features of the geometric shape of the scene (the normal ν_p to the surface), but it is also affected by its *global* shape. Thus with such a modeling, if we want to exploit radiance to recover the shape of the scene, then we have to deal with global equations and not only with local equations as it is the case with the classical modelings of the Shape From Shading problem.

In order to simplify the problem and to remove this global dependency, Lions, Rouy and Tourin [19] assume that for all the points of the surface, *all the light sources* located on the normal hemisphere *are visible*. More rigorously, they assume that

$$supp(R_L) \cap Hemi_{\nu_p} \subset \mathbf{C}_{\mathcal{S},p} \quad (3)$$

where for a vector $\mathbf{q}$ in $\mathbb{R}^3$, the hemisphere $Hemi_{\mathbf{q}}$ is the set $\{\nu \in \mathbb{S}^2 \mid \langle \mathbf{q}, \nu\rangle \geq 0\}$, and where the support $supp(.)$ of a function is the closure of the set on which this function does not vanish. In other words, Lions et al. assume that there are no self-shadows. Also, such an assumption simplifies strongly the problem because we have then $R_L(\nu) = 0$ outside of $\mathbf{C}_{\mathcal{S},p}$ and so $\int_{\mathbf{C}_{\mathcal{S},p}} \langle \nu, \nu_p\rangle\, R_L(\nu)\, d\nu = \int_{\mathbb{S}^2} \langle \nu, \nu_p\rangle\, R_L(\nu)\, d\nu$ which completely removes the global dependency of the radiance with respects to the whole shape.

Here, in this paper, we want to consider *full* ambient illumination $R_L(\nu)dL(\nu)$; i.e. we want to deal with R_L distribution such that $supp(R_L) = \mathbb{S}^2$. In other words, light comes from all directions. In such a case, Lions' assumption (3) is equivalent to assume that the surface is convex which is really a too restrictive assumption. *Also in this paper, we completely relax assumption* (3) *assumed in [19] while completely*

braving self-shadows difficulties. In return, in order to keep a tractable problem, we assume that the *ambient illumination is uniform*, i.e.

$$R_L(\nu)dL(\nu) = R_0 dL, \text{ where } R_0 \in \mathbb{R}.$$

Without lose of generality we can then also assume that $R_0 = 1$.

3 Mathematical Formulation of the Shape From Ambient Shading Problem

3.1 Imaging Equation

The Shape From Shading problem is the following: given a gray level image I (the data), we want to find the surface(s) $\mathcal{S}$ which generate an identical image to I. By assuming that the brightness of a pixel x of the image is equal to the radiance of the point $\pi_{\mathcal{S}}^{-1}(x)$ of the surface viewed in x (see [14] to understand the validity of this assumption), the SFS problem then consists in solving equation $I(x) = R_{\mathcal{S}}(\pi_{\mathcal{S}}^{-1}(x))$. With the above modeling assumptions on the lighting and the reflectance, this equation them becomes

$$I(x) = \int_{\mathbf{C}_{\mathcal{S},p}} \langle \nu, \nu_p \rangle^+ \, d\nu, \tag{4}$$

where ν_p is the outward-pointing normal vector to the surface $\mathcal{S}$ at the point $p = \pi_{\mathcal{S}}^{-1}(x)$. This equation is called the *"imaging equation"*. Also, in the sequel we are going to assume that the data image I corresponds with an image of a scene verifying our modeling assumptions. In particular we have $0 \leq I(x) \leq \pi$; see [14].

3.2 Mathematical Formulation as a Partial Differential Equation

Let $\mathfrak{D}$ be a closed set of $\mathbb{R}^2$ representing the domain of definition of the input image (data); for example, $\mathfrak{D}$ is the rectangular domain $[0, X] \times [0, Y]$. The intensity of the input image is modelled as a function I from $\mathfrak{D}$ into the closed interval $[0, \pi]$, by

$$I : \mathfrak{D} \longrightarrow [0, \pi] : x \mapsto I(x).$$

We assume that the surface $\mathcal{S}$ representing the scene can be explicitly parameterized by a function S from $\mathfrak{D}$ into $\mathbb{R}^3$ by $x \mapsto S(x)$;

$$\mathcal{S} = \{S(x); \quad x \in \mathfrak{D}\}.$$

For simplicity, we assume that the camera performs an *orthographic projection* of the scene. With this hypothesis, it is natural to define the surface $\mathcal{S}$ by

$$\mathcal{S} = \{(x_1, x_2, u(x_1, x_2)); \quad (x_1, x_2) \in \mathfrak{D}\}.$$

So, if the plane $(0, \overrightarrow{x_1}, \overrightarrow{x_2})$ represents the retinal plane then $|u(x)|$ is the distance of the points $S(x)$ in the scene to the camera (see [21]). For such a surface $\mathcal{S}$, the outward-pointing normal vector $\nu_{S(x)}$ is given by

$$\nu_{S(x)} = \frac{1}{\sqrt{1 + |\nabla u(x)|^2}}(-\nabla u(x), 1).$$

Following [24, 23, 21], we could assume that the camera is a pinhole. As demonstrated in [24, 21] the mathematical study as well as the numerical issues of the problem would be a just little more sophisticated in this case, but all the results are the exactly same.

With the orthographic camera model, the *imaging equation* becomes then the following Partial Differential Equation (PDE)

$$I(x) = \int_{\mathbf{C}_{u,(x,u(x))}} \left\langle \frac{1}{\sqrt{1+|\nabla u(x)|^2}}(-\nabla u(x), 1)\ ,\ \nu \right\rangle^+ d\nu, \tag{5}$$

where $\mathbf{C}_{u,p}$ denote $\mathbf{C}_{\mathcal{S},p}$ (the surface $\mathcal{S}$ is represented by the function u).

So, according to our modelling, the shape from ambient shading problem consists of resolving the PDE (5), given an image I. This equation is a first order stationary **integro-partial differential** equation. It is a **global** PDE of the form:

$$H(x, u(x), \nabla u(x), u(.)) = 0, \quad \forall x \in Int(\mathfrak{D}). \tag{6}$$

The numerical and theoretical study of the solutions of these kind of equation is done by using some representations: the "Hamiltonians". To equation (5), we can associate the following Hamiltonians equally:

$$H_1(x,t,p,u) = \int_{\mathbf{C}_{u,(x,t)}} \langle \frac{1}{\sqrt{1+|p|^2}}(-p,1), \nu\rangle^+ d\nu - I(x)$$

or $H_2(x,t,p,u) = -H_1(x,t,p,u)$.

4 Theoretical Study of the Shape From Ambient Shading Equation

In the previous section we have formulated the SFAS problem as the one of solving equation (5). Now we are going to theoretically analyze this equation. More exactly, we are going to consider the problem of the uniqueness of its solution. Actually, we are going to show that the solution is not unique and then we are going to characterize all the solutions.

Let us emphasize that the interests of such an analysis is twofolds. First characterizing all the solutions is an essential prerequisite if we want to be able to numerically compute a solution and to understand what we get (contribution from the algorithmic/computational point of view). Second, this allows to understand the complexity and the ambiguities contained in this shading information (contribution from the vision point of view).

4.1 An Intrinsic Ambiguity

First, let us remind that the radiance verifies

$$0 \leq R_{\mathcal{S}}(p) \leq \pi, \qquad p \in \mathcal{S}$$

and that $\mathbf{C}_{\mathcal{S},p} \subset Hemi_{\nu_p}$. Also, it is easy to verify that

$$R_{\mathcal{S}}(p) = \pi \ \text{ iff } \ \mathbf{C}_{\mathcal{S},p} = Hemi_{\nu_p}.$$

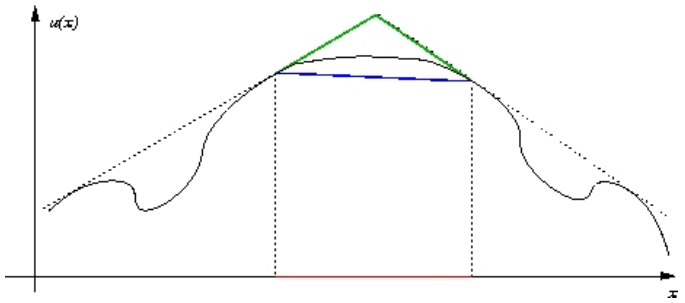

Figure 1: Example of multiple solutions in dimension 2 when the image contains a subset of pixels having the maximal intensity. Any curve between the blue and the green curves, and which is concave on the set of points with maximal intensity generates the same image as the one generated by the initial black curve.

Now, let us consider a completely white image with a maximal intensity; i.e. we consider the case of the specific image I such that $I(x) = \pi$ for all pixels x in the image domain $\mathfrak{D}$. With such an image, the solutions of equation (4) verify then $\mathbf{C}_{\mathcal{S},p} = Hemi_{\nu_p}$ for all the points p on the surface. Therefore, according to the representation of section 3.2, for all pixels (x), the whole surface stays below the tangent plane to the surface at the point $(x, u(x))$. So the solutions u of PDE (5) are concave (so the shape itself is convexe). Since inversely all concave functions generate such a white image then we can conclude that the set of solutions is the one of all the concave functions. With such an image, the SFAS problem is then ill-posed because the considered image can be generated by a number of different surfaces: in other words the solution is not unique. Also, this difficulty does not only appear in this extreme case: in fact it appears as soon as the image contains a subset of pixels having the maximal intensity. Figure 1 illustrates this fact in dimension 2. In this figure, pixels with maximal intensity (i.e. the pixels such that $I(x) = \pi$) are drawn in red. The green curve corresponds with maximal solution when the blue one gives the minimal solution. Any curve between these two curves and which is concave on the set of points with maximal intensity generates the same image as the one generate by the black curve.

In the following sections, we are going to show that this condition is actually minimal, that is to say that the solution is unique iff there are no subsets of pixels having the maximal intensity. Also, when the solutions are multiple, then a solution is characterized by its values on this subset.

4.2 Uniqueness Result and Characterization of the solutions

In this section we are going to show that the solutions of the SFAS problem are charaterized by their values on the subset of the $\{x \mid I(x) = \pi\}$. To the end, let us define $\Omega = \{x \mid I(x) < \pi\}$ and let us complete the equation

$$H(x, u(x), \nabla u(x), u) = 0, \forall x \in \mathfrak{D} \tag{7}$$

by some Dirichlet boundary conditions on $\complement\Omega = \mathfrak{D} - \Omega = \{x \in \mathfrak{D} \mid I(x) = \pi\}$. In other words, we assume that we know the height of the solution on this subset. Mathematically, the considered equation then becomes

$$\begin{cases} H(x, u(x), \nabla u(x), u) = 0, & \forall x \in \Omega, \\ u(x) = \varphi(x) & \forall x \in \complement\Omega. \end{cases} \tag{8}$$

For mathematical conveniences, we also assume that the brightness image I is continuous (then Ω is an open subset of $\mathfrak{D}$) and that the intensity is maximal on the boundary of the image (in other words, we assume that $\overline{\Omega} \subset \mathcal{I}nt\ \mathfrak{D}$).

We can ever since state the uniqueness theorem

Theorem 4.1 (Uniqueness)**.** *If u and v are two C^1 solutions to equation* (8) *then $u = v$ on $\mathfrak{D}$.*

This theorem which immediately follows from the maximum principle stated and proved in the sequel (theorem 4.3), ensures that there exists at most a unique C^1 solution to equation (8). Also, this provides a characterization of the set of the solutions of equation (7): a solution of equation (7) on the whole image is characterized by its values on the subset $\mathcal{C}\Omega$ (the region where $I(x) = \pi$). If there are no region in the image on which $I(x) = \pi$, then we will have a unique solution to equation (7) (complemented by a Dirichlet constraint on the boundary of the image domain).

From the computer vision point of view, this uniqueness result can be interpreted as follows. Assuming we know the height of the solution on the subset of maximal intensity, $\{x \mid I(x) = \pi\}$, i.e. on the region on which shading does not give any information, then there exists a unique solution to the Shape From Ambient Shading problem. As a consequence, on the other parts of the image, the ambient shading information allows by itself to recover (characterize) the original surface from which the image has been generated.

Practically it is not possible to know the solution in the region of maximal intensity. But we can imagine using other techniques like photometric stereo or stereovision to first estimate the height of the solution on the subset $\{x \mid I(x) = \pi\}$ so that we have a unique solution.

Remark: About maximal solutions and degenerate equations:
It is interesting to remark that contrary to the classical SFS equations of the form $H(x, \nabla u) = 0$ for which we can define and characterize the maximal solution in the degenerate cases [22], here there clearly does not exist maximal solution, when the equation is degenerate (i.e. when there exists x in Ω such that $I(x) = \pi$). Intuitively, it seems that there exists a minimal solution which can coincide with a minimal super-solution.

Definition 4.2. Let $u \in C^1(\mathfrak{D}, \mathbb{R})$.
u is a sub-solution of equation (7) iff $\forall x \in \mathfrak{D}$, $H(x, u(x), \nabla u(x), u) \leq 0$.
u is a super-solution of equation (7) iff $\forall x \in \mathfrak{D}$, $H(x, u(x), \nabla u(x), u) \geq 0$.

Theorem 4.3 (Maximum Principle)**.** *Let $u, v \in C^1(\mathfrak{D}, \mathbb{R})$, respectively a* **sub***solution, and a* **super***solution of equation (7). If we assume that $u \leq v$ on $\mathcal{C}\Omega$, then $u \leq v$ on $\mathfrak{D}$.*

Proof. Let us consider $\delta = \max_{\mathfrak{D}}(u - v)$. Let us denote

$$M_\delta = \{x \in \mathfrak{D} \mid u(x) - v(x) = \delta\}.$$

Since u and v are continuous on the compact set $\mathfrak{D}$, M_δ is a closed subset of $\mathbb{R}^2$.

We can consider two cases:

1. $M_\delta \cap \mathcal{C}\Omega \neq \emptyset$.
   In this case there exists $x_0 \in M_\delta \cap \mathcal{C}\Omega$. Since $x_0 \in \mathcal{C}\Omega$, we have $u(x_0) \leq v(x_0)$. So $\delta \leq 0$. Therefore $\forall x \in \mathfrak{D},\ u(x) - v(x) \leq \max_{\mathfrak{D}}(u - v) = \delta \leq 0$. i.e. $u \leq v$ on $\mathfrak{D}$.

2. $M_\delta \cap \complement\Omega = \emptyset$.
   In this case, the closed subset (of $\mathbb{R}^2$) M_δ is a subset of the open subset (of $\mathbb{R}^2$) Ω.

   - Since $u,\ v \in C^1(\mathfrak{D}, \mathbb{R})$, $M_\delta \subset \mathcal{I}nt\ \mathfrak{D}$ and $\delta = \max u - v$, then, for all x in M_δ, then $\nabla u(x) = \nabla v(x)$.
   - For $u \in C^1(\mathfrak{D}, \mathbb{R})$ and $x \in \mathfrak{D}$, we denote

$$T_{u,x} = \left\{ y \in \mathfrak{D} \mid \frac{\vec{XY}}{|\vec{XY}|} \in \partial \mathbf{C}_{u,(x,u(x))}, \right. \\ \left. \text{where } \vec{XY} = (x, u(x)) - (y, u(y)) \right\}.$$

   - We have the following lemma and propositions:

     Lemma 4.4. *Let $u_1, u_2 : \Omega \to \mathbb{R}$ and $x_0 \in \Omega$ be such that $u_1 \geq u_2$ and $u_1(x_0) = u_2(x_0)$. Then $\mathbf{C}_{u_1,(x_0,u_1(x_0))} \subset \mathbf{C}_{u_2,(x_0,u_2(x_0))}$.*

     Proof. Trivial! □

     Proposition 4.5. *If $x_0 \in M_\delta$ then $T_{u,x_0} \subset M_\delta$.*

     Proof. – Since $v(x_0) = u(x_0) - \delta$ and for all x we have $v(x) \geq u(x) - \delta$, then by lemma 4.4 we have

$$\mathbf{C}_{v,(x_0,v(x_0))} \subset \mathbf{C}_{u-\delta,(x_0,u(x_0)-\delta)}.$$

     – *By contradiction*, let assume that there exists y in T_{u,x_0} s.t. $y \notin M_\delta$. We have then trivially $v(y) > u(y) - \delta$, so by continuity we have

$$\mathbf{C}_{v,(x_0,v(x_0))} \subsetneq \mathbf{C}_{u-\delta,(x_0,u(x_0)-\delta)}.$$

     – Since $u, v \in C^1(\Omega)$ and $u - v$ is maxima at x_0, then

$$\nabla v(x_0) = \nabla u(x_0) = \nabla[u - \delta](x_0).$$

     Let us denote $p = \nabla u(x_0) = \nabla v(x_0)$. We have

$$H_1(x_0, v(x_0), p, v) = \int_{\mathbf{C}_{v,(x_0,v(x_0))}} \langle \frac{1}{\sqrt{1+|p|^2}}(-p, 1), \nu \rangle^+ \, d\nu - I(x_0) \tag{9}$$

$$\begin{aligned} H_1(x_0, u(x_0), p, u) &= H_1(x_0, u(x_0) - \delta, p, u - \delta) \\ &= \int_{\mathbf{C}_{u-\delta,(x_0,u-\delta(x_0))}} \langle \frac{1}{\sqrt{1+|p|^2}}(-p, 1), \nu \rangle^+ \, d\nu - I(x_0) \end{aligned} \tag{10}$$

     Since the expression inside the integral sign is non-negative then by the previous item, we have

$$H_1(x_0, v(x_0), p, v) < H_1(x_0, u(x_0), p, u).$$

– u being a sub-solution of H_2, we obtain

$$H_1(x_0, v(x_0), p, v) < 0$$

which contradicts the assumption that v is a super-solution.

□

Proposition 4.6. *For all x in $\mathfrak{D}$, for all y in $T_{u,x}$, $\mathbf{C}_{u,(x,u(x))} \subset \mathbf{C}_{u,(y,u(y))}$. We have also:*

– *Let y in $T_{u,x}$, if $\mathbf{C}_{u,(x,u(x))} = \mathbf{C}_{u,(y,u(y))}$, then $\overrightarrow{(x,u(x))(y,u(y))} = (y,u(y)) - (x,u(x))$ is in the tangent plane to u at x.*

– *If for all y in $T_{u,x}$, $\mathbf{C}_{u,(x,u(x))} = \mathbf{C}_{u,(y,u(y))}$, then $\mathbf{C}_{u,(x,u(x))} = Hemi_{\nabla u(x)}$.*

• Let us denote

$$V_u : \mathfrak{D} \to \mathbb{R},\ x \mapsto \int_{\mathbf{C}_{u,(x,u(x))}} 1 d\nu.$$

Proposition 4.7. *If $u \in C^1(\mathfrak{D}, \mathbb{R})$, then V_u is continuous on $\mathfrak{D}$.*

• Let $x_1 = \arg\max_{x \in M_\delta} V_u(x)$. Since $x_1 \in M_\delta$, Proposition 4.5 involves $\forall y \in T_{u,x_1}$, $y \in M_\delta$ and so, by definition of x_1, $V_u(y) \leq V_u(x_1)$. By Proposition 4.6, we have $\mathbf{C}_{u,(x_1,u(x_1))} \subset \mathbf{C}_{u,(y,u(y))}$. So it follows that $\mathbf{C}_{u,(x_1,u(x_1))} = \mathbf{C}_{u,(y,u(y))}$. Therefore, by last item of Proposition 4.6, we have $\mathbf{C}_{u,(x_1,u(x_1))} = Hemi_{\nabla u(x_1)}$, and so

$$H_1(x_1, u(x_1), \nabla u(x_1), u) = \pi - I(x_1).$$

Since we have assumed that $x_1 \in \Omega$, we have $\pi - I(x_1) > 0$. Then $H_1(x_1, u(x_1), \nabla u(x_1), u) > 0$. This leads to a contradiction since we have assumed initially that u is a sub-solution of (7).

□

5 Approximation Scheme And Numerical Algorithm

In section 3 we have written the SFAS problem as the resolution of a partial differential equation of the form $H(x, u(x), \nabla u(x), u) = 0$. The problem being ill-posed, we had then to add some Dirichlet boundary conditions on $\complement\Omega = \mathfrak{D} - \Omega$ (section). This last step which allows to characterize the solutions is fundamental if we want to understand what we can expect to compute and if we want test the relevance of any algorithm.

In order to compute a reliable numerical solution to this equation, we use mathematical literature dealing with Hamilton-Jacobi equations. The key point consists then in designing approximation schemes which are **monotone** [9, 4].

5.1 Monotonic Scheme

For convenience let us remind the reader of the definition of an approximation scheme. An approximation scheme is a functional equation of the form

$$T(h, x, u^\rho) = 0 \qquad \forall x \in \overline{\Omega};$$

where T is a real function defined on $\mathcal{M} \times \overline{\Omega} \times B(\overline{\Omega})$; $\mathcal{M} = \mathbb{R}^+ \times \mathbb{R}^+$ and $h \in \mathcal{M}$ define the size of the mesh that is used in the corresponding numerical algorithms; $B(\overline{\Omega})$ is the space of bounded functions defined on the set $\overline{\Omega}$. u^ρ is the unknown (u^ρ is a function). Also, we are interested in the solution u^ρ of the scheme T.
For $h_1, h_2 \in \mathbb{R}^+$, we write $h = (h_1, h_2)$. If $h_1 = h_2$, we let $h = h_i \in \mathbb{R}^+$. Also, we (mis)use the notation "$\forall h > 0$" which stands for "$\forall h \in \mathcal{M}$ such that $h_1 > 0$ and $h_2 > 0$".
Generally, we say that a scheme is monotone if for all $h \in \mathcal{M}$ and $x \in \overline{\Omega}$, the function $T(h, x, \cdot) : B(\overline{\Omega}) \to \mathbb{R}$ is monotone [i.e. if for all $y \in \overline{\Omega}$, $u(y) \geq v(y)$, then $T(h, x, u) \geq T(h, x, v)$; resp. $T(h, x, u) \geq T(h, x, v)$].
Following [4], we introduce the representation S of a scheme T as

$$S(h, x, u^\rho(x), u^\rho) = 0 \qquad \forall x \in \overline{\Omega}, \tag{11}$$

where

$$\begin{array}{rccc} S: & \mathcal{M} \times \overline{\Omega} \times \mathbb{R} \times B(\overline{\Omega}) & \longrightarrow & \mathbb{R} \\ & (h, x, t, u) & \longmapsto & S(h, x, t, u). \end{array}$$

Note that a representation of a scheme is also a scheme. This last mathematical object allows to exploit and to take full advantage of the tools developed by Barles and Souganidis [4] which roughly speaking needs that the scheme is monotonic with respect to all the values of u up to the value at one point, generally $u(x)$. We then isolate $u(x)$ from the other values of u. Also, let us stress that the result demonstrated by Barles and Souganidis [4] is optimal for large class of (static as well as evolutive) Hamilton-Jacobi equations.
The introduction of representations is also a way to simplify computations. In effect, the representation of a scheme $T(h, x, u^\rho) = 0$ by a scheme of the form

$$S(h, x, u^\rho(x), u^\rho) = 0$$

suggests an iterative algorithm for computing a numerical approximation of the solution of the scheme. Given u^n (the approximation of u^ρ at step n), and a point x of $\overline{\Omega}$, the associated algorithm consists in solving the equation

$$S(h, x, t, u^n) = 0 \tag{12}$$

with respect to t. A solution of (12) is the updated value of u^n at x.
Here, we are then going to use the definition of monotonicity given by Barles and Souganidis in [4]:

Definition 5.1 (monotonicity). The scheme $S(h, x, u^\rho(x), u^\rho) = 0$ defined in $\overline{\Omega}$, is monotone if $\forall h \in \mathcal{M}, \forall x \in \overline{\Omega}, \forall t \in \mathbb{R}$ and $\forall u, v \in B(\overline{\Omega})$,

$$u \leq v \quad \Longrightarrow \quad S(h, x, t, u) \geq S(h, x, t, v)$$

(the scheme is non-increasing with respect to u).

The interest of the monotonicity is twofold.

1) Complemented by some other basic assumptions [monotonicity with respect to t, existence of a subsolution, bound for the subsolutions], this property is the key property which ensures that the scheme is stable (existence of the solution and of a upper bound), that the iterative algorithm (mentioned above) is well-posed and that the computed numerical approximations converge toward the solution of the scheme see [21, 24].

2) Combined with some stability and consistency properties, the monotonicity ensures that the solutions of the scheme converge toward the viscosity solution of the considered equation when the mesh vanishes see [4]. Also, if Barles and Souganidis [4] only deal with Hamilton-Jacobi equations of the type $H(x, u(x), \nabla u(x), D^2u(x)) = 0$, their result has been extended to various I-PDEs, see [1, 2, 3, 16].

In the sequel, we are then going to design a monotonic approximation scheme for the SFAS problem in order to take advantage of all these benefits.

5.2 Monotonic Scheme For SFAS problem

For readability, in the sequel we denote $H_{u,t}$ the function defined by

$$H_{u,t}(x, p) = H(x, t, p, u).$$

Let us remind that for the SFAS problem, the Hamiltonian we are considering is

$$H_{u,t}(x, p) = \int_{\mathbf{C}_{u,(x,t)}} \langle \frac{1}{\sqrt{1 + |p|^2}}(-p, 1), \nu \rangle^+ \, d\nu - I(x).$$

One can verify easily that $\mathbf{C}_{u,(x,t)}$ (ordered by the inclusion) is decreasing with respect to u and increasing with respect to t. Also, it follows that $H_{u,t}$ verifies exactly the same monotonic properties. In other respects, in order to get a consistent approximation scheme, we have to replace ∇u (represented by the variable p in the above Hamiltonian) in the PDE by one of its numerical approximations (finite differences). The difficult is then to find such a discretization in a way which keep the above monotonic properties.

In [25, 21], Prados et al. propose some generic approximation schemes for solving the SFS equations in the case where the light source is punctual, i.e. when $dL(\nu)$ is a Dirac. The approximation schemes are based on the rewriting of the Hamiltonian in the optimal control framework. For punctual light sources, they are consistent, stable and monotonic. Unfortunately the direct transposition of the approximation schemes of Prados et al., in the case where $dL(\nu)$ is continuous (in particular for SFAS), does not yield in a monotonic scheme.

In order to get a monotonic scheme, we take inspiration on *Lax-Friedrichs scheme* for conservation laws [10, 9]. We chose:

$$S(h, x, t, u) = H_{u,t}(x, \mathbf{D}u(x)) - \theta \, \mathbf{L}u^t(x), \tag{13}$$

where $\mathbf{D}u(x)$ is the vector obtained by a centered discretization of $\nabla u(x)$, more precisely, the i^{th} component of $\mathbf{D}u(x)$ is

$$[\mathbf{D}u(x)]_i = \frac{u(x + h_i \overrightarrow{e_i}) - u(x - h_i \overrightarrow{e_i})}{2 \, h_i}$$

and where $\mathbf{L}u^t(x)$ is the classical discretization of the Laplacian $\Delta u(x)$ (in which one replaces $u(x)$ by t), i.e.

$$\mathbf{L}u^t(x) = \sum_{i=1..N} \frac{u(x + h_i \overrightarrow{e_i}) + u(x - h_i \overrightarrow{e_i}) - 2t}{h_i^2}.$$

Nevertheless, still this scheme is not necessarily monotonic. To satisfy this property, we need to find an adequate value for θ.

1. Monotonicity of $S(h, x, t, u)$ with respect to $u(x)$.
   The scheme is not dependent on $u(x)$.

2. Monotonicity of $S(h, x, t, u)$ with respect to $u(y)$, for all $y \neq x$ and $y \neq x \pm h_i\overrightarrow{e_i}$, $\forall i$.
   Let us fix $y \neq x$ and $y \neq x \pm h_i\overrightarrow{e_i}$, $\forall i$. In the right part of the equation (13), only $H_{u,t}(x, p)$ depends on $u(y)$. Also, for all (x, p) and t, the function $u \mapsto H_{u,t}(x, p)$ is non-increasing. The monotonicity of $S(h, x, t, u)$ with respect to $u(y)$ follows immediately.

3. Monotonicity of $S(h, x, t, u)$ with respect to $u(y)$, for $y = x + h_i\overrightarrow{e_i}$ or $y = x - h_i\overrightarrow{e_i}$, $i \in [1..N]$.
   By differential calculus, one can easily verify that a sufficient condition to ensure this property is $\max_{i=1..N} h_i \left|\partial_{p_i} H_{u,t}(x, Dz)\right| \leq 2\theta$ and that $\left|\partial_{p_i} H_{u,t}(x, p)\right| \leq 2\sqrt{2}\pi$, see appendix A.

In the case where $h_1 = h_2 := h$, the scheme (13) is then monotonic as soon as

$$\theta \geq \sqrt{2}\pi h.$$

Also, to limit the smoothing due to the Laplacian term introduced in the scheme (term which can be interpreted as a regularization), θ must be the smallest as possible. We then choose

$$\boxed{\theta_{opt} = \sqrt{2}\pi h}$$

($\theta_{opt} = 2h$ if we draw upon some experimental results).

In other respects, under the assumptions of section 4.2, one can easily verify that any deep enough function is a subsolution of the scheme (13) (because the visibility cone is then extremely small). Moreover, the subsolutions are necessarily bounded by the function corresponding to convex hull defined by the Dirichlet boundary constraints. Since the scheme is also increasing with respect to t and verifies

$$\lim_{t \to +\infty} S(h, x, t, u) \geq 0$$

then theorems 3.1 and 3.5 of [21], ensure that the scheme (13) is stable and the approximations computed by associated iterative algorithm converge toward the solution of the scheme.
Practically, we can start from any subsolution and we have just to update the surface with scheme (13) until the convergence. Finally, our scheme being also consistent with the SFAS I-PDE, relying on Barle and Souganidis theorem [4] and its extensions to various I-PDEs, we can conjecture that the computed approximations converge toward the "viscosity solution" of the I-PDE [2]. This guarantees the reliability of our numerical approximations toward the theoretical solution of our problem.

6 Numerical Experiments

6.1 Implementation

We focus here on the numerical results obtained by the algorithm associated to the scheme (13). As described in section 5.1, approximation schemes of the form (11)

[2] Barle and Souganidis result also needs a strong uniqueness property, but we already have proved a similar result in section 4.

suggest an iterative numerical algorithm, whose updating step (at point x) involves solving the equation in t

$$S(h, x, t, u) = 0,$$

where u is the approximation of the whole solution at the previous step (see [21]). Here the solution of associated equation $H_{u,t}(x, \mathbf{D}u(x)) - \theta\ \mathbf{L}u^t(x) = 0$ (equation in t) is not explicit. Nevertheless, this equation can be trivially rewritten as a fixed point equation $t = g(t)$ which can be numerically solved by an iterative method. For example, in dimension 2D with $h = h_1 = h_2$, the fixed point equation is $t = \frac{1}{4}\left(\sum_{i=1,2}(u(x + h\overrightarrow{e_i}) + u(x - h\overrightarrow{e_i})) - \frac{h^2}{\theta}H_{u,t}(x, \mathbf{D}u(x)\right)$. Practically we only process some iterations $t_{n+1} = g(t_n)$ which systematically converge after less than 5 iterations [we assign t_0 to the previous value of $u(x)$]. The numerical scheme starts with a subsolution as a very steep valley such that visibility is closed to 0 for all points in domain.

In other respects, to evaluate the visibility cone of a point on the surface we use the perpective projection from OpenGL. We take 6 projections on each face of a cube around the point. The visibility cone is then evaluated using these 6 projection images.

To update the value of the solution at one pixel, we render 6 images to evaluate visibility cone and we need around 4 fixed point iterations to converge the inner iterative loop. So for an $M \times N$ image, the overall complexity of the algorithm for ensuring its convergence is $24(MN)^2$. This is computationally too expensive to be run on a single PC. We are then use distributed computing (Message Passing Interface or MPI) to evaluate this on up to 20 processors. The depth estimation algorithm is still very time consuming. It generally takes up to 10 hours for a 48×48 image on 20 processors.

6.2 Experiments

To test our algorithm, we consider some scenarios for which the problem is well-posed. In other words, we limit the computation domain to a subset of $\Omega = \{x \mid I(x) < \pi\}$. This computation domain is delimited by the red box in the corresponding figures. On the other part of the image domain, we enforce Dirichlet Boundary Conditions.

We start by simulating the ambient shading image for the $\sin(x)\sin(y)$ surface and we use it as the input image to our numerical algorithm. For this first test, we restrict the computation domain to a subset on which the surface is concave. We set $u_0(x)$ as a steep valley such that $u_0(x)$ is a subsolution. As shown in Figure 2 , the computed iterative solution converges nicely toward the original surface. It is interesting to notice that, in this specific setup, the obtained results are extremely stable with respect to the θ parameter. In practice, we can choose θ much smaller than $\sqrt{2}\pi h$ (up to a a critical value for θ). Also the smaller is θ, the faster is the algorithm. The obtained result is also more accurate. Actually, this flexibility is due to the fact that the sup of $|\partial_{p_i} H_{u,t}(x, p)|$ during all the process is much smaller than the upper bound mathematically estimated (bound which must fit to the most critical case).

In the second test, we want to extend the computation domain to both concave and convex areas. To remove the ambiguity due to points with maximal intensity, we reduce the intensity of the image by placing the $\sin(x)\sin(y)$ surface in a box, i.e. surrounded by four walls of a cube with the roof open. In this test, the algorithm converges toward the solution in both concave and convex regions. Nevertheless, as shown Figure 3, when the reconstruction is very accurate in the convex region, there is a significative error in the concave region.

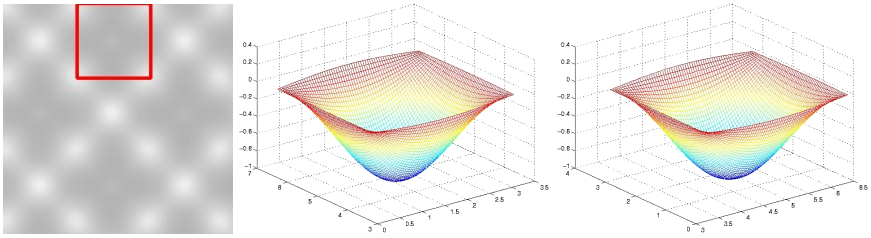

Figure 2: Left: image generated by the $\sin x * \sin y$ surface with $h = 0.05$ and region of interest where we run the algorithm; middle: original surface (ground-truth) on the region interest; right: surface reconstructed by our algorithm (result).

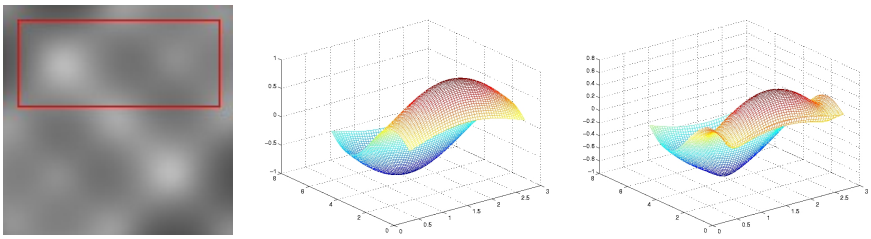

Figure 3: Left: image generated by the $\sin x * \sin y$ surface with $h = 0.05$ inside a cubical box and region of interest where we run the algorithm; middle: original surface (ground-truth) on the region of interest; right: surface reconstructed by our algorithm (result).

	min value	max value	L_1 errors	L_2 errors	L_∞ errors
$\sin x \sin y$, Fig. 2	-0.999707	0.066750	0.006191	0.009792	0.033867
$\sin x \sin y$ in box, Fig. 3	-0.999707	0.999568	0.188896	0.240712	0.372564

Table 1: Errors for the first two tests.

Table 1 shows the minimum and maximum values of the original surfaces in the regions of interest (where algorithm is applied). It also shows the L_1, L_2 and L_∞ errors. The top row shows the errors for the first test ($\sin(x)\sin(y)$ surface) illustrated in Figure 2. The second row shows the errors for $\sin(x)\sin(y)$ surface inside a box; it corresponds with the result of Figure 3. In our experiments, we have used the L_1 error for convergence test.

Actually in the second test, one can understand the large error on the concave region as a result of the introduction of the regularization term (which was needed to make the scheme monotonic). To further analyze this effect, we focus on the concave part and we perform the following two experiments.

To validate our feeling, we first run our algorithm with an input image containing the regularization term. More exactly, we use

$$\tilde{I}(x) = \int_{\mathbf{C}_{u,(x,u(x))}} \langle \frac{1}{\sqrt{1+|\mathbf{D}u(x)|^2}}(-\mathbf{D}u(x),1), \nu\rangle^+ \, d\nu - \theta \, \mathbf{L}u(x)$$

	Min Value	Max Value	L_1 Error	L_2 Error	L_∞ Error
without regularization	-0.999707	0.999568	0.186037	0.189434	0.207331
with regularization	-0.999707	0.999568	0.065627	0.067900	0.078941

Table 2: Errors by adding the regularization term in the input image.

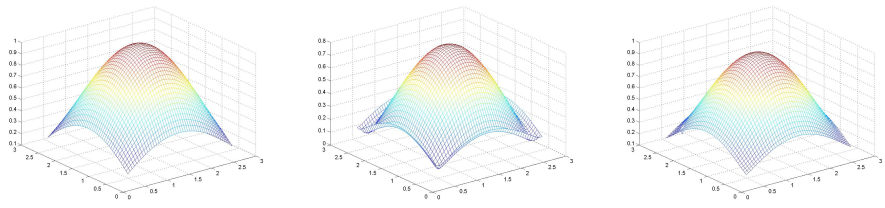

Figure 4: Above: $sinx * siny$ image with regularization and region of interest where we run the numerical scheme. Below: Results of the numerical scheme with (right) and without (left) regularization in input image.

mesh sizes (h)	min values	max values	L_1 errors	L_2 errors	L_∞ errors
$h = 0.2$	0.151647	0.999147	0.504147	0.526644	0.658852
$h = 0.1$	0.151647	0.999147	0.358676	0.371685	0.424875
$h = 0.08$	0.151647	0.999147	0.270054	0.276862	0.308127
$h = 0.05$	0.145665	0.999568	0.186037	0.189434	0.207331
$h = 0.04$	0.138681	0.999883	0.151427	0.153691	0.166671

Table 3: Errors with smaller and smaller h.

as input in our algorithm. So practically, the algorithm computes the solution of equation $\int_{\mathbf{C}_{u,(x,u(x))}} \langle \frac{1}{\sqrt{1+|\mathbf{D}u(x)|^2}}(-\mathbf{D}u(x),1),\nu\rangle^+ \, d\nu - \tilde{I}(x) - \theta\, \mathbf{L}u(x) = 0$ and the computed solution should then exactly coincides with the original surface. We then make this test with the $\sin x \sin y$ surface inside the box (with a computation domain reduced to the concave part). As shown in table 2 and Figure 4, the algorithm is now able to recover the exact surface. We observe that the regularization term had an effect of $\pm 15\%$ of the visibility in the concave region of the surface. Since the laplacian is negative in this region, the surface seems to have a lower visibility than actual in the concave region using the approximation scheme (13). This then explains the behavior of the computed solutions.

Finally, since the regularization parameter θ is linearly dependent with the size of the mesh h, then the regularization effect should reduce when the size of the mesh vanishes. We then redone the second test ($\sin x \sin y$ surface inside a box, with the same reduced computation domain as previously) with smaller and smaller mesh sizes: $h = 0.2, 0.1, 0.08, 0.05, 0.04$. Also, as we can see in Figure 5 and Table 3, the computed approximations actually converge towards the original surface when the mesh size is reduced. In addition to confirm the above assertion, this also validates our methodology and our theory which ensures to get a well-posed algorithm whom the output convergences toward the continuous solution when the mesh vanishes.

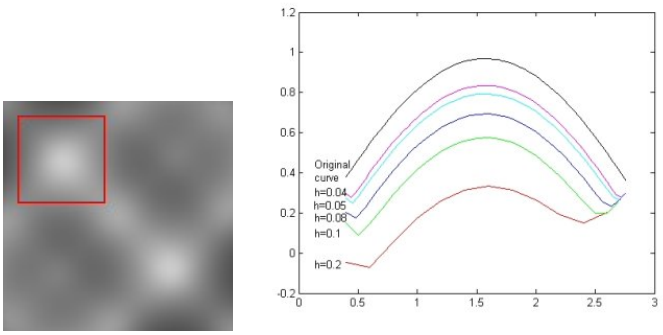

Figure 5: Reconstruction with different mesh sizes h.

7 Conclusion and Future Work

In computer vision, lighting is generally modeled very roughly (when it is modeled!); for example, the authors model it by using a finite number of punctual light sources complemented by an ambient term which is reduced to the addition of a constant value to the radiance of the scene. Our initial idea was to consider more realistic models of lighting, in particular for the ambient light, and to show that this can be relevant in the computer vision fields. In order to really unsdertand what happens, we then consider the Shape From Shading problem which is a good toy problem with which one can develop mathematical theory. Also, in this thesis, via the Shape From Shading problem and a rigorous theoretical and algorithmic study of this problem, we managed to show that ambient shading contains information which can be really exploited in 3D shape reconstruction, whereas it is ignored and not modeled in the computer vision community (and so it is also never exploited!).

More pragmatically, this report states the first theoretical result for the non-local Shape From Ambient Shading I-PDE: characterization of the solutions. Also we propose a rigorous numerical algorithm allowing to approximate the solutions of this equation.

The problem we consider here being quite difficult, our endeavor suggests various prospective work. From the mathematical point of view, since generally the considered I-PDE do not have solutions in the classical sense, it would be relevant to study the problem in a weak framework as the one of the notion of viscosity solutions created by Crandall and Lions [8]. The notion of viscosity solutions being well defined and studied only for local PDEs, this will need to generalize this notion and to made-up a new mathematical theory. From the algorithmic point of view, it would be nice to provide a monotonic approximation scheme without the regularization term which provides unpleasant effects in our experiments. From the computer vision point of view, it would be interesting to exploit the ambient shading in other problems such as, for example, photometric stereo and stereovision.

Acknowledgment

We would like to thank warmly Fabio Camilli and Espen Jakobsen for the various discussions we had around this subject.

A Monotonicity of $S(h,x,t,u)$ with respect to u

Let us consider here the monotonicity of $S(h,x,t,u)$ with respect to $u(y)$, for $y = x + h_i\overrightarrow{e_i}$ or $y = x - h_i\overrightarrow{e_i}$, $i \in [1..N]$.

For all (x,p) and t, the function $u \mapsto H_{u,t}(x,p)$ is non-increasing. So $S(h,x,t,u)$ is non-increasing with respect to $u(x + h_i\overrightarrow{e_i})$ (resp. $u(x - h_i\overrightarrow{e_i})$) as soon as, for $x,\ t,\ u$ fixed, the function $z \mapsto H_{u,t}(x,Dz) - \theta\ Lz$ is non-increasing, where Dz and Lz correspond with the expression of $\mathbf{D}u(x)$ and $\mathbf{L}u(x)$ in which we have replaced $u(x + h_i\overrightarrow{e_i})$ (resp. $u(x - h_i\overrightarrow{e_i})$) by z. A sufficient condition is then

$$\nabla_p H_{u,t}(x,Dz)\cdot(0,...,0,\frac{1}{2\ h_i},0,...,0) - \theta\frac{1}{h_i^2} \leq 0$$

(resp. $-\nabla_p H_{u,t}(x,Dz)\cdot(0,...,0,\frac{1}{2\ h_i},0,...,0) - \theta\frac{1}{h_i^2} \leq 0$).
Therefore, $S(h,x,t,u)$ is non-increasing with respect to all $u(x + h_i\overrightarrow{e_i})$ and $u(x - h_i\overrightarrow{e_i}),\ \forall i = 1..N$ as soon as for all i,

$$h_i\,|\partial_{p_i} H_{u,t}(x,Dz)| \leq 2\theta$$

i.e. as soon as

$$\max_{i=1..N}\ h_i\,|\partial_{p_i} H_{u,t}(x,Dz)|\ \leq 2\theta. \tag{14}$$

Now, let us give some explicit values for θ. One can prove that

$$|\partial_{p_i} H_{u,t}(x,p)| \leq 2\sqrt{2}\pi.$$

Proof. Summary we have $\partial_{p_i} H_{u,t}(x,p) = \int_{\mathbf{C}_{u,(x,t)}} \partial_{p_i}[\Psi\circ G](p)\,d\nu$, where $\Psi : \mathbb{R} \to \mathbb{R} : a \mapsto a^+$ and G is the function defined by $G : p \mapsto \left\langle \frac{1}{\sqrt{1+|p|^2}}(-p,1), \nu \right\rangle$. Also we have

$$|\partial_{p_i} H_{u,t}(x,p)| \leq \int_{\mathbf{C}_{u,(x,t)}} |\partial_{p_i}[\Psi\circ G](p)|\,d\nu \leq \int_{\mathbf{C}_{u,(x,t)}} |\partial_{p_i} G(p)|\,d\nu.$$

In other respects, let us denote $g(p) = \frac{1}{\sqrt{1+|p|^2}}(-p,1)$. We have

$$\partial_{p_i} G(p) = \langle \partial_{p_i} g(p), \nu\rangle$$

and then by Cauchy-Schwarz

$$|\partial_{p_i} G(p)| \leq |\partial_{p_i} g(p)||\nu| = |\partial_{p_i} g(p)|$$

Also $|\partial_{p_i} g(p)| \leq \sqrt{2}$. Thus we have $|\partial_{p_i} H_{u,t}(x,p)| \leq 2\sqrt{2}\pi$.
(Experimentally, it seems that $|\partial_{p_i} H_{u,t}(x,p)| \leq 4$. Nevertheless we do not have a mathematical proof of that as of now.) □
□

References

[1] O. Alvarez and A. Tourin. Viscosity solutions of nonlinear integro-differential equations. *Annales de l'institut Henri Poincaré (C) Analyse non linéaire*, 13(3):293–317, 1996.

[2] A. L. Amadori. *Differential and integro-differential nonlinear equations of degenerate parabolic type arising in the pricing of derivatives in incomplete market*. PhD thesis, University of Roma I - La Sapienza, 2001.

[3] L. Amadori, K. H. Karlsen, and C. La Chioma. Nonlinear degenerate integropartial differential evolution equations related to geometric levy processes and applications to backward stochastic differential equations. *GSSR*, 76(2):147–177, April 2004.

[4] G. Barles and P.E. Souganidis. Convergence of approximation schemes for fully nonlinear second order equations. *Asymptotic Analysis*, 4:271–283, 1991.

[5] D. Burton and L. Davis. The shape of shadows. Technical Report TR-147, Univ of Texas at Austin, July 1980.

[6] P. Cavanagh and Y. G. Leclerc. Shape from shadows. *Journal of Experimental Psychology: Human Perception and Performance*, 15:3–27, 1989.

[7] J. Clark and L. Wang. Active shape-from-shadows with controlled illuminant trajectories. *Int. J. Comput. Vision*, 43(3):141–166, 2001.

[8] M. G. Crandall and P. L. Lions. Viscosity solutions of hamilton-jacobi equations. *Transactions of the American Mathematical Society*, 277(1):1–43, 1983.

[9] M. G. Crandall and P. L. Lions. Two approximations of solutions of Hamilton-Jacobi equations. *Mathematics of Computation*, 43(167):1–19, 1984.

[10] M. G. Crandall and A. Majda. Monotone difference approximations for scalar conservation laws. *Mathematics of Computation*, 34(149):1–21, January 1980.

[11] M. Daum and G. Dudek. On 3-d surface reconstruction using shape from shadows. In *CVPR*, pages 461–468, 1998.

[12] J-D. Durou, M. Falcone, and M. Sagona. A survey of numerical methods for shape from shading. Research report 2004-2-R, IRIT, January 2004.

[13] M. Hatzitheodorou. Shape from shadows: a hilbert space setting. *J. Complex.*, 14(1):63–84, 1998.

[14] B.K. Horn. *Robot Vision*. mit-press, 1986.

[15] B.K. Horn and M.J. Brooks, editors. *Shape from Shading*. The MIT Press, 1989.

[16] E. R. Jakobsen and K. H. Karlsen. A maximum principle for semicontinuous functions applicable to integro-partial differential equations. *NoDEA Nonlinear Differential Equations Appl.*, 13:137–165, 2006.

[17] M. S. Langer and H. H. Bulthoff. Depth discrimination from shading under diffuse lighting. *Perception*, 29(6):649–660, 2000.

[18] M. S. Langer and S. W. Zucker. Shape from shading on a cloudy day. *Journal of Optical Society of America*, 11:467–478, 1994.

[19] P.-L. Lions, E. Rouy, and A. Tourin. Shape-from-shading, viscosity solutions and edges. *Numer. Math.*, 64:323–353, 1993.

[20] S. Nayar, K. Ikeuchi, and T. Kanade. Shape from interreflections. *Int. J. Comput. Vision*, 6(3):173–195, 1991.

[21] E. Prados. *Application of the theory of the viscosity solutions to the Shape From Shading problem*. PhD thesis, Univ. of Nice-Sophia Antipolis, 2004.

[22] E. Prados, F. Camilli, and O. Faugeras. A viscosity method for shape-from-shading without boundary data. Technical report, INRIA, 2004.

[23] E. Prados and O. Faugeras. "Perspective Shape from Shading" and viscosity solutions. In *Proceedings of ICCV'03*, volume 2, pages 826–831, October 2003.

[24] E. Prados and O. Faugeras. A generic and provably convergent shape-from-shading method for orthographic and pinhole cameras. *International Journal of Computer Vision*, 65(1/2):97–125, nov 2005.

[25] E. Prados and O. Faugeras. Shape from shading: a well-posed problem ? In *Proceedings of the IEEE Conference on Computer Vision and Pattern Recognition (CVPR'05), San Diego, California*, volume II, pages 870–877. IEEE, jun 2005.

[26] Emmanuel Prados, Nitin Jindal, and Stefano Soatto. A Non-Local Approach to Shape From Ambient Shading. In *2nd International Conference on Scale Space and Variational Methods in Computer Vision (SSVM'09)*, Lecture Notes in Computer Science series, pages 696–708, Voss, Norway, 2009. Springer-Verlag.

[27] A.J. Stewart and M. S. Langer. Towards accurate recovery of shape from shading under diffuse lighting. *IEEE Transactions on Pattern Analysis and Machine Intelligence*, 19(9):1020–1025, 1997.

[28] Y.L Tian, H.T. Tsui, S.Y. Yeung, and S. Ma. Shape from shading for multiple light sources. *Journal of the Optical Society of America*, 16(1):36–52, January 1999.

[29] T. Wada, H. Ukida, and T. Matsuyama. Shape from shading with interreflections under proximal light source-3D shape reconstruction of unfolded book surface from a scanner image. In *Proceedings of ICCV'95*, June 1995.

[30] J. Yang, D. Zhang, N. Ohnishi, and N. Sugie. Determining a polyhedral shape using interreflections. In *CVPR '97: Proceedings of the 1997 Conference on Computer Vision and Pattern Recognition (CVPR '97)*, page 110. IEEE Computer Society, 1997.

[31] Y. Yu and J. Chang. Shadow graphs and surface reconstruction. In *In European Conference on Computer Vision*, pages 31–45. Springer-Verlag, 2002.

[32] R. Zhang, P.-S. Tsai, J.-E. Cryer, and M. Shah. Shape from Shading: A survey. *IEEE Transactions on Pattern Analysis and Machine Intelligence*, 21(8):690–706, August 1999.

Contents

1 Introduction **3**

2 Modeling of The Problem **4**
2.1 Reflectance Assumptions 4
2.2 Lighting Assumptions 5
2.3 Resulting Radiance 6

3 Mathematical Formulation of the Shape From Ambient Shading Problem **7**
3.1 Imaging Equation 7
3.2 Mathematical Formulation as a Partial Differential Equation 7

4 Theoretical Study of the Shape From Ambient Shading Equation **8**
4.1 An Intrinsic Ambiguity 8
4.2 Uniqueness Result and Characterization of the solutions 9

5 Approximation Scheme And Numerical Algorithm **12**
5.1 Monotonic Scheme 12
5.2 Monotonic Scheme For SFAS problem 14

6 Numerical Experiments **15**
6.1 Implementation 15
6.2 Experiments 16

7 Conclusion and Future Work **19**

A Monotonicity of $S(h, x, t, u)$ with respect to u **20**

Centre de recherche INRIA Grenoble – Rhône-Alpes
655, avenue de l'Europe - 38334 Montbonnot Saint-Ismier (France)

Centre de recherche INRIA Bordeaux – Sud Ouest : Domaine Universitaire - 351, cours de la Libération - 33405 Talence Cedex
Centre de recherche INRIA Lille – Nord Europe : Parc Scientifique de la Haute Borne - 40, avenue Halley - 59650 Villeneuve d'Ascq
Centre de recherche INRIA Nancy – Grand Est : LORIA, Technopôle de Nancy-Brabois - Campus scientifique
615, rue du Jardin Botanique - BP 101 - 54602 Villers-lès-Nancy Cedex
Centre de recherche INRIA Paris – Rocquencourt : Domaine de Voluceau - Rocquencourt - BP 105 - 78153 Le Chesnay Cedex
Centre de recherche INRIA Rennes – Bretagne Atlantique : IRISA, Campus universitaire de Beaulieu - 35042 Rennes Cedex
Centre de recherche INRIA Saclay – Île-de-France : Parc Orsay Université - ZAC des Vignes : 4, rue Jacques Monod - 91893 Orsay Cedex
Centre de recherche INRIA Sophia Antipolis – Méditerranée : 2004, route des Lucioles - BP 93 - 06902 Sophia Antipolis Cedex

Éditeur
INRIA - Domaine de Voluceau - Rocquencourt, BP 105 - 78153 Le Chesnay Cedex (France)
http://www.inria.fr
ISSN 0249-6399